UC Irvine
UC Irvine Previously Published Works

Title
Characterization of long-range functional connectivity in epileptic networks by neuronal spike-triggered local field potentials

Permalink
https://escholarship.org/uc/item/49m9g71d

Journal
Journal of Neural Engineering, 13(2)

ISSN
1741-2560

Authors
Lopour, Beth A
Staba, Richard J
Stern, John M
et al.

Publication Date
2016-04-01

DOI
10.1088/1741-2560/13/2/026031

Peer reviewed

eScholarship.org Powered by the California Digital Library
University of California

Characterization of long-range functional connectivity in epileptic networks by neuronal spike-triggered local field potentials

Beth A. Lopour[1], Richard J. Staba[2], John M. Stern[2], Itzhak Fried[3], Dario L. Ringach[4,5]

[1] *Department of Biomedical Engineering, University of California, Irvine, CA 92697 USA*

[2] *Department of Neurology*

[3] *Department of Neurosurgery and Semel Institute for Neuroscience and Human Behavior*

[4] *Department of Neurobiology*

[5] *Department of Psychology, University of California, Los Angeles, CA 90095 USA*

Corresponding Author

beth.lopour@uci.edu

3120 Natural Sciences II

University of California

Irvine, CA 92697

Abstract

Objective

Quantifying the relationship between microelectrode-recorded multi-unit activity (MUA) and local field potentials (LFPs) in distinct brain regions can provide detailed information on the extent of functional connectivity in spatially widespread networks. These methods are common in studies of cognition using non-human animal models, but are rare in humans. Here we applied a neuronal spike-triggered impulse response to electrophysiological recordings from the human epileptic brain for the first time, and we evaluate functional connectivity in relation to brain areas supporting the generation of seizures.

Approach

Broadband interictal electrophysiological data were recorded from microwires adapted to clinical depth electrodes that were implanted bilaterally using stereotactic techniques in six presurgical patients with medically refractory epilepsy. MUA and LFPs were isolated in each microwire, and we calculated the impulse response between the MUA on one microwire and the LFPs on a second microwire for all possible MUA/LFP pairs. Results were compared to clinical seizure localization, including sites of seizure onset and interictal epileptiform discharges.

Main results

We detected significant interictal long-range functional connections in each subject, in some cases across hemispheres. Results were consistent between two independent datasets, and the timing and location of significant impulse responses reflected anatomical connectivity. However, within individual subjects, the spatial distribution of impulse responses was unique. In two subjects with clear seizure localization and successful surgery, the epileptogenic zone was associated with significant impulse responses.

Significance

The results suggest that the spike-triggered impulse response can provide valuable information about the neuronal networks that contribute to seizures using only interictal data. This technique will enable testing of specific hypotheses regarding functional connectivity in epilepsy and the relationship between functional properties and imaging findings. Beyond epilepsy, we expect that the impulse response could be more broadly applied as a measure of long-range functional connectivity in studies of cognition.

1 Introduction

Functional connectivity analysis using microelectrode recordings can provide detailed insight into brain networks by quantifying the relationship between multi-unit activity (MUA) and local field potential (LFP) in distinct locations. These methods are common in studies of cognition using non-human animal models. For example, spike-field coherence and the spike-triggered average of the LFP have been used to study attention (Gregoriou et al., 2009; Womelsdorf et al., 2006), memory (Pesaran et al., 2002), and vision (Jin et al., 2011; Nauhaus et al., 2009; Swadlow et al., 2002). A related measure, called the impulse response, incorporates a pre-whitening step during which spatiotemporal autocorrelations within spike trains are factored out (Einevoll et al., 2013). It has been used to analyze lateral connectivity in the visual cortex (Nauhaus et al., 2012) and the accuracy of LFP estimates based on local MUA (Rasch et al., 2009). While microelectrode recordings in humans are becoming increasingly common, they are still rare and chiefly carried out during the presurgical diagnostic evaluation of epilepsy (Engel et al., 2005). Human recordings provide a unique opportunity not only to study cognitive processing and behavior (Cash and Hochberg, 2015; Fried et al., 2014), but also to investigate basic mechanisms of epilepsy.

The pathological networks that contribute to epileptic seizures can be extensive and are thus interpreted as global changes in the organization of the brain (Engel et al., 2013). Temporal lobe epilepsy (TLE) can affect the default mode network (Haneef et al., 2012; Pittau et al., 2012; Voets et al., 2012) and cause changes both ipsilateral and contralateral to the seizure onset zone (Bettus et al., 2009; Holmes et al., 2014; Maccotta et al., 2013). While some general conclusions can be drawn, there is evidence that these epileptic networks are patient-specific (Luo et al., 2014). This wide variability and broad spatial extent makes identification a challenge, and therefore there is a lack of understanding of the pathological functional networks that support the generation of seizures. We aim to address this need by assessing patient-specific functional connectivity via microwire recordings that were adapted to the distal tip of clinical depth electrodes and implanted stereotactically in presurgical patients with medically refractory epilepsy.

In order to quantify the spatial distribution of functional connections with respect to the seizure onset zone, we computed the neuronal spike-triggered impulse response between the MUA and LFP for all microwire pairs. Using interictal data, we are able to detect significant long-range

connections in each subject that, in some cases, occurred between hemispheres. The resulting networks are unique for each patient. In two subjects with clear seizure localization and successful surgery, the location of significant impulse responses was consistent with the epileptogenic zone. This technique may provide valuable information about the long-range functional connections that contribute to seizures. For example, the impulse response could be used to test specific hypotheses regarding hippocampal connectivity in epilepsy (Haneef et al., 2014; Holmes et al., 2014), and the functional properties could be related to imaging findings such as hippocampal sclerosis. Further, the estimation of functional connectivity presented here can be done with approximately twenty minutes of interictal electrophysiological data and does not require waiting for or inducing seizures.

2 Materials and methods

2.1 Participants

We collected interictal data from six consecutive patients (2 female, 4 male; average age 38.6 +/- 14 years) who were undergoing presurgical evaluation for the treatment of medically refractory epilepsy. The study was approved by the Medical Institutional Review Board at the University of California, Los Angeles, and each subject provided informed consent to participate in the study. All subjects were awake and sitting up in a hospital bed during the recording. Two sets of data were obtained for each patient, separated by a rest period of several minutes, and the average length of each dataset was 11.98 minutes (min 9.14, max 14.17) and 9.78 minutes (min 8.25, max 10.92).

2.2 Electrophysiology

Each subject was bilaterally implanted with 8-12 depth electrodes as a means of localizing epileptic activity in preparation for surgery. In total, we analyzed data from 480 platinum-iridium microwires (8 microwires from 60 depth electrodes) that were 40 μm in diameter. The microwires protruded from the tip of each depth electrode and were used to record both multi-unit activity (MUA) and extracellular local field potential (LFP) activity.

The depth electrode locations were chosen based exclusively on clinical criteria and typically included structures in the temporal lobe (amygdala, hippocampus, entorhinal cortex, parahippocampal gyrus, superior temporal gyrus) and the frontal lobe (orbitofrontal cortex, anterior cingulate gyrus, middle cingulate, supplementary motor area). In total, 288 microwires

were positioned in mesial temporal lobe and 192 were in mesial frontal lobe structures. Before implantation, each patient received whole brain magnetic resonance imaging (MRI). After implantation, electrode placement was verified by co-registering a computed tomography (CT) scan to the MRI.

2.3 Data collection and preprocessing

The data were recorded at 30 kHz using a 128-channel Neuroport system (Blackrock Microsystems, Salt Lake City, UT). An amplitude threshold for multi-unit activity (MUA) was determined relative to the bandpass filtered (0.3-6 kHz) baseline activity, and neuronal spikes were automatically detected whenever the threshold was exceeded. Data for LFP analysis was downsampled to 2 kHz using the MATLAB "resample" function. A bipolar montage within each bundle of 8 microwires (channel 1 − channel 2, channel 2 − channel 3, etc. yielding 8 bipolar signals) was used for the analysis to ensure that all neural responses were local to the depth electrode and to prevent artificial correlation due to a common reference.

The data contained interictal EEG spikes and intermittent electronic and movement-related artifacts that introduced strong correlations between large groups of channels over short periods of time. While it has been shown that the relationship between neuronal spiking and interictal epileptiform discharges shows considerable variation (Keller et al., 2010; Wyler et al., 1982), this activity may lead to spurious functional connections between brain regions. Therefore, these sections of data were excluded from the analysis using the following procedure: We first calculated the correlation coefficients across all channels using 1-second windows of raw LFP data and an overlap of 900ms. We then calculated the sum of the absolute value of the correlation coefficients, excluding self-correlations and correlations between bipolar pairs that contained a common channel. This represented the overall level of correlation across channels for that time window; artifacts caused this value to be unnaturally high. The windows with the top 10% of correlation levels were excluded from analysis. The windows selected by this algorithm corresponded nicely to visually-identified artifacts and interictal discharges (see Supplementary Figure 1 for examples from each subject). Overall, this is a conservative approach to the impulse response analysis since the strongest correlations are excluded from the calculation.

2.4 Broadband impulse response analysis

Here we aim to measure the functional connectivity of the human brain by assessing the correlation between MUA in one region and LFP in a different region. This is commonly done via calculation of the spike-triggered LFP; for monosynaptic feedforward connections, this can be interpreted as a measurement of the postsynaptic activation due to a single spike. However, positive spatiotemporal correlations within the MUA can cause spurious results when analyzing the spike-triggered LFP (Figure 1) (Einevoll et al., 2013). Therefore, we instead calculate the impulse response between the MUA and LFP, which incorporates a pre-whitening step for the MUA. The pre-whitening enables one to, effectively, deconvolve the measured input (spike times based on MUA) from the output at distant electrode sites (the LFP). Mathematically, this is based on a model of connectivity where spikes are convolved by post-synaptic convolution kernels (at the population or ensemble level) to produce the LFP. These convolution kernels correspond to the impulse response functions.

Each microwire measured both MUA and LFP. The impulse response was calculated from the MUA in each microwire to the LFP in all other microwires. Therefore, n microwires produced n^2 broadband impulse response measurements. To make the calculation tractable, the LFP was further downsampled to 500 Hz. The multi-unit spike trains (MUA) were convolved with a Gaussian window at 2 kHz and then resampled at 500 Hz to match the LFP. A low-pass filter (<100Hz) was applied to isolate the LFP, and a notch filter (55-65Hz) removed electrical line noise.

The impulse response was calculated using correlation analysis via the MATLAB function “cra” over the time interval [-0.5, 0.5] seconds relative to each multi-unit spike. Due to the 500 Hz sampling rate, each impulse response was 501 points long. A tenth order pre-whitening filter was used. The “cra” function provides three outputs: ir (the estimated impulse response with no negative lags), R (which contains the lag indices, the covariance functions, and the correlation function), and cl (the 99% confidence level associated with the calculation). Note that a properly scaled version of the correlation function (in the output R) is equivalent to the estimated impulse response, except it includes negative lag times. We therefore used a scaling factor of S = ir(end)/R(end,4)*fs, so our estimate of the impulse response was R(:,4)*S. The associated confidence interval was cl*fs. Other Matlab functions (impulse, impulseest) were tested and provided similar results, but the cra function was found to be the most computationally efficient.

2.5 Amplitude-based impulse response analysis

After completing the calculations using the broadband LFP signal (<100 Hz), we repeated them using the amplitude of the LFP at ten individual frequencies between 4 Hz and 100Hz. This allowed us to identify activity that was both phase-locked (resulting from deconvolution of the raw time-series) and non-phase-locked (resulting from deconvolution of the frequency-specific amplitude of induced responses) to the MUA.

The amplitude of the LFP was isolated via wavelet convolution, using the free WaveLab toolbox for MATLAB (http://statweb.stanford.edu/~wavelab/). We performed a continuous wavelet transform using the function "CWT_Wavelab" with a five-cycle wavelet and parameters nvoice = 10, scale = 4, and oct = 6. Then the magnitude of the resulting complex vector ("abs" in MATLAB) was used to calculate the instantaneous amplitude of the signal.

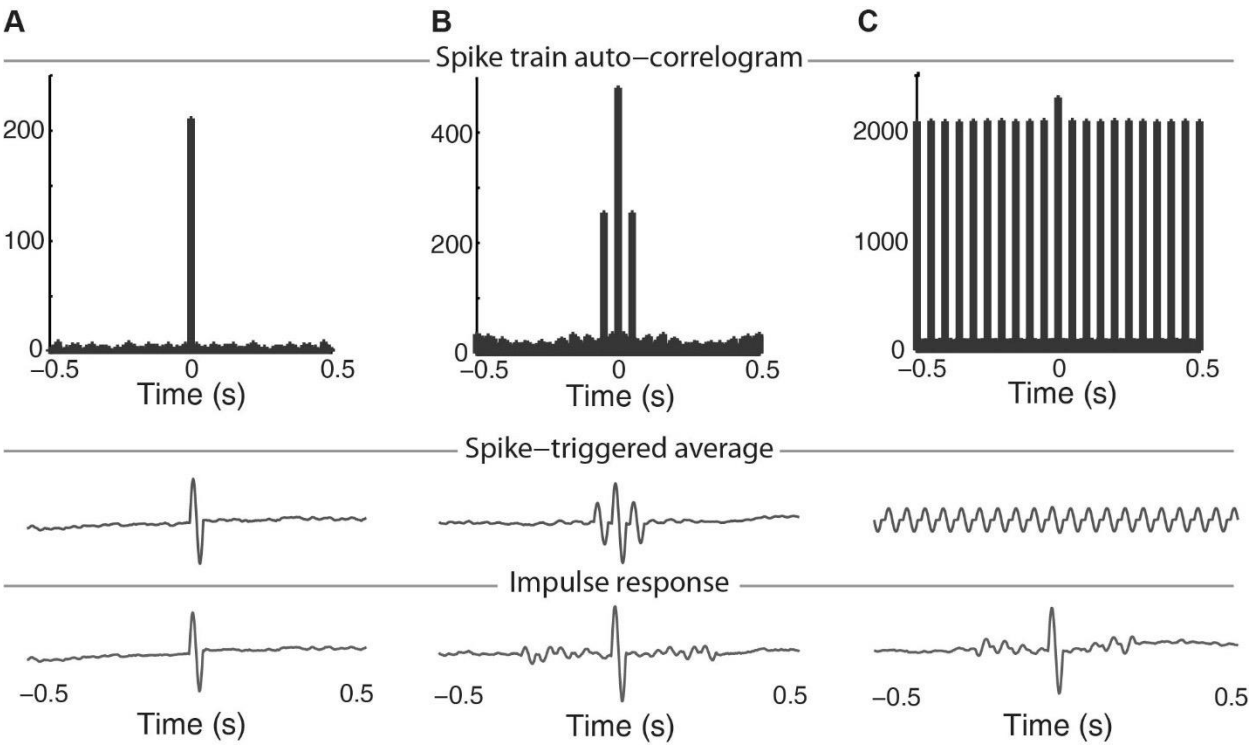

Figure 1. The impulse response is related to the spike-triggered average. Three artificial spike trains were compared to a simulated LFP signal, designed such that each spike was associated with a simple biphasic response in the LFP. The spike train auto-correlogram is shown for each spike train (top row), and the spike-triggered average (middle row) and impulse response (bottom row) were calculated for each spike/LFP pair. **(A)** When the spike train is temporally uncorrelated, the spike-triggered average and impulse response produce the same result. **(B, C)** When

the spikes are temporally correlated to one another (e.g. indicative of rhythmic spiking), the spike-triggered average is negatively affected. However, the impulse response is able to recover the simulated biphasic response. This demonstrates the advantage of choosing impulse response analysis over a simple spike-triggered average. Panels B and C represent low and high levels of temporal autocorrelation among the spikes.

Ten frequencies were analyzed at log-base-2 intervals from 4 Hz to 90.51 Hz. To speed up computation of the impulse response, the amplitude data was resampled at 10 times the frequency of interest before doing the calculation (e.g. to study the impulse response based on the amplitude at 32 Hz, a sampling frequency of 320 Hz was used). The MUA was resampled at the same rate after convolving with a Gaussian window as described above. Each impulse response was 301 samples long and centered on the time of the neuronal spike. Due to the difference in sampling rate, the length of the impulse response in seconds varied as a function of frequency (333 ms for 90.51Hz, 470 ms for 64 Hz, 940 ms for 32 Hz, 1.88 seconds for 16 Hz, and so forth).

As in the broadband analysis, the impulse response was calculated using the MATLAB function "cra" with a pre-whitening filter of order 10.

2.6 Significance testing

The impulse responses were calculated independently for each dataset (two per patient). The significance of each impulse response was based on two criteria: 1) the peak value of the response in both datasets must exceed a threshold (1.25 times the MATLAB confidence interval as discussed below) and 2) the paired responses from the two datasets (for the same MUA/LFP channels) must be correlated with $R > 0.8$ and $p < 0.01$. This ensures that the magnitude of the response is significantly higher than chance levels and that the MUA/LFP relationship is stable. When a response is deemed to be significant, it is an indication that the MUA and LFP are correlated, and it is thus a measure of functional connectivity between the two brain regions where the signals were measured.

Because MATLAB does not provide documentation regarding the calculation of the confidence level, we verified the validity of this approach by comparing it to a confidence level calculated via permutation resampling. We used permutation resampling to calculate baseline values for 88 impulse responses, based on MUA from 8 channels and LFP from 11 channels. We disrupted the

temporal relationship between MUA and LFP by shifting the multi-unit spike trains by a random amount, and then we recalculated the impulse response. This process was repeated 100 times per channel pair. We calculated the maximum value of the impulse response for each iteration and used the distribution of maximum values to determine a 95% confidence level. The MATLAB-provided confidence level was higher (more strict) than the permutation resampling confidence level in 77 out of 88 channel pairs. Therefore, the use of MATLAB's confidence level for significance testing is a valid and conservative approach.

3 Results

3.1 Impulse response measurements reveal functional connectivity between distant brain regions

Using pairs of MUA and LFP from distinct brain regions, we identified significant impulse responses in each subject (Figure 2). The responses did not require spatial proximity between the MUA and LFP. In some cases, the MUA was correlated to the LFP in a different lobe of the brain (e.g. temporal vs. frontal) and in other cases the two signals were in different hemispheres. Interestingly, there were cases where both the broadband impulse response and amplitude-based impulse response were significant (Figure 2A,D), as well as cases where only the broadband response (Figure 2C,F) or only the amplitude-based impulse response was significant (Figure 2B,E). A significant broadband result requires that the LFP is phase-locked to the MUA, while the amplitude-based response captures frequency-specific activity without the phase-locking requirement. These results suggest that the impulse response can be used as a measure of functional connectivity between distant brain regions and that both phase-locked and non-phase-locked activity contribute to this relationship.

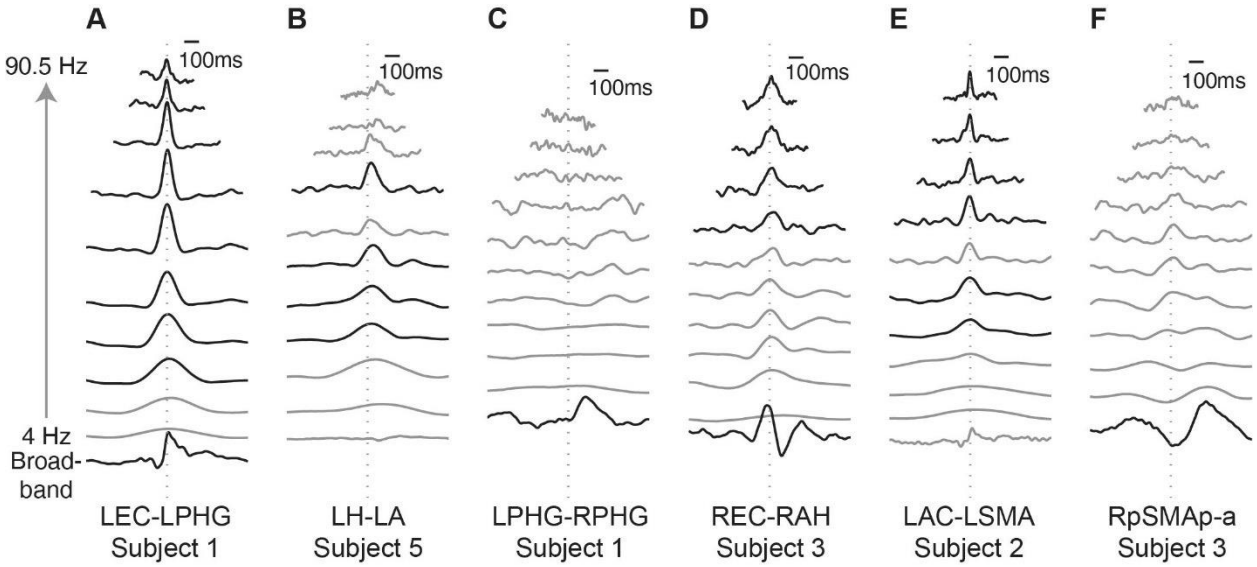

Figure 2. Significant impulse responses occurred in each subject across distinct brain regions. Sample measurements of significant impulse responses are shown for both the broadband and amplitude-based measures. Broadband responses are in the bottom row, and the center frequency for the amplitude-based responses is ordered from bottom (low frequencies) to top (high frequencies). Significant responses are shown in black and non-significant responses are shown in gray. The subject number and MUA-LFP pair are listed below each result, and the vertical dashed line represents the peak of the multi-unit spike. Each response has been divided by the confidence level to normalize the amplitude. In some cases, both the broadband and amplitude-based impulse responses are significant (Subfigures 2A,D). In other cases, only the amplitude-based impulse response (Subfigures 2B,E) or the broadband impulse response (Subfigures 2C,F) is significant. The responses in each category share similar characteristics, although they come from different patients and brain structures. Note that all connections are between unique brain structures (there are no self-connections) and connections to the contralateral hemisphere are demonstrated.

Key: Prefix of R/L indicates right/left; suffix of a/p indicates anterior/posterior; A = amygdala, AC = anterior cingulate, AH = anterior hippocampus, H = hippocampus, EC = entorhinal cortex, PHG = parahippocampal gyrus, (p)SMA = (pre) supplementary motor area

In general, the broadband impulse responses were more likely to be significant than those based on the amplitude at a specific frequency (Figure 3). While the number of significant broadband impulse responses is not a function of frequency (Figure 3, gray with crosshatch), the percent of those that are significant based on both the amplitude and the broadband measures (Figure 3, gray) and the percent that are significant based on the amplitude but not the broadband measure (Figure 3, black) vary with frequency. For impulse responses based on amplitude, there are peaks in the number of significant connections at 32 Hz and 90.51 Hz. Note that this figure includes

self-connections, where the MUA and LFP are recorded from the same brain structure and sometimes from the same microwire. This type of connection is more likely to become significant as the frequency increases due to the low-frequency component of the spike waveform contained within the LFP (see Section 4 and Figure 5); this is the likely cause of the peak at 90.51 Hz.

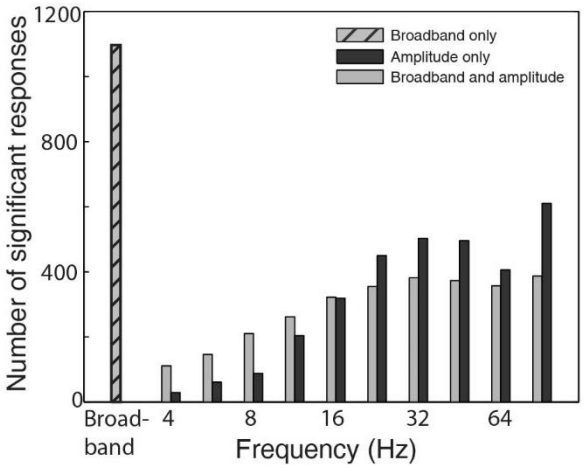

Figure 3. The number of significant impulse responses varies with frequency. Here the connections are divided based on which type of LFP signal produced a significant result: broadband (gray with crosshatch), amplitude at a specific frequency but not the broadband signal (black), or both broadband and amplitude (gray). For example, the black traces in Figures 2A and 2D would be included in the gray bars here, because both the frequency-based and broadband impulse responses are significant. The black traces in Figures 2B and 2E are significant based only on frequency, and would be included in the black bars here.

3.2 Timing and location of broadband impulse responses reflects anatomical connectivity

Across all subjects, the significant broadband impulse responses suggest connectivity patterns that were consistent with known anatomical characteristics. As expected, MUA and LFP from the same brain structure had the greatest incidence of significant impulse responses (12.95% of self-connections were significant, across all six subjects, n=4032 possible connections). Ipsilateral connections within the same lobe of the brain (e.g. left amygdala to left hippocampus or right supplementary motor area to right anterior cingulate) had the second highest rate of significance (3.97%, n=7424). Inter-hemispheric connections were most likely to be significant if they were between analogous structures (e.g. left amygdala to right amygdala, 3.16%, n=2752)

or lobes (e.g. left temporal lobe structure to right temporal lobe structure, 1.74%, n=10752). Inter-hemispheric connections between different lobes (e.g. left temporal lobe to right frontal lobe) were very rarely significant (0.27%, n=8064). Ipsilateral connections to a different lobe of the brain (e.g. left temporal lobe to left frontal lobe) were also relatively rare (0.82%, n=7808). Results from individual subjects are generally consistent with these patterns of significance (Figure 4A).

It is important to note that within the categories mentioned above, significant connections tend to be clustered in specific brain structures and do not reflect all known anatomical connections. For example, in Subject 1, 6.6% of all ipsilateral same lobe connections were significant. However, if we narrow the focus to connections within the left temporal lobe, we find that 13.9% were significant. This is compared to 3.1% within the right temporal lobe, and <0.05% within the left frontal lobe. While there are known anatomical connections between temporal lobe structures (e.g. amygdala, hippocampus, entorhinal cortex), the impulse response may be strong only between a subset of these structures or only in one hemisphere. This suggests that the impulse response is not measuring pure anatomical connectivity. Rather, we hypothesize that it is related to the pathological epileptic network in each subject (see Section 3.4).

Further, the timing of the peak of the impulse response appears to reflect the spatial proximity of the two brain structures used in the calculation (Figure 4B). For self-connections and ipsilateral connections between structures in the same lobe of the brain, the peak of the impulse response tends to occur near the peak of the MUA (Figure 4B, top row; median values are 16ms and 34ms, respectively). These are contrasted with connections between the left and right temporal lobes or the left and right frontal lobes, where the peak of the impulse response is delayed relative to the peak of the MUA (Figure 4B, bottom left; median value 108ms). This is presumably due to the complex, polysynaptic nature of the connection. Note that there were not enough significant ipsilateral connections between the temporal and frontal lobes to draw a robust conclusion about the timing (Figure 4B, bottom right; median value 4ms).

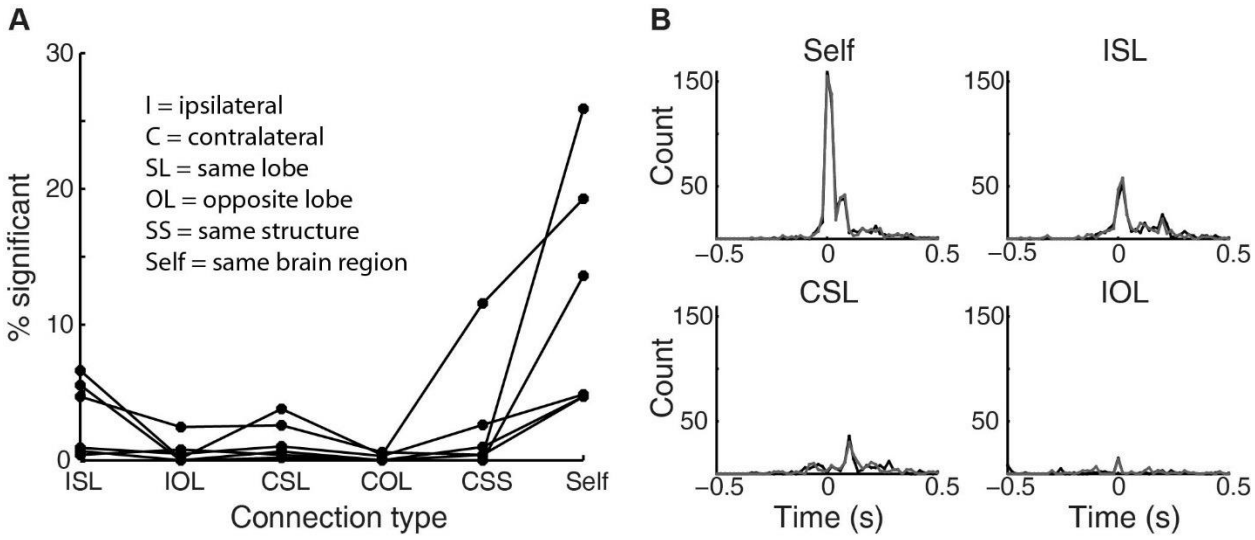

Figure 4. Significant broadband impulse responses mirror anatomical connectivity. (A) Percentage of significant broadband impulse responses, categorized by connection type, for all six subjects. Results for a single subject are connected by black lines. Self-connections are the most likely to be significant, followed by ISL and CSS connections, and then CSL connections. IOL and COL connections are less likely to be significant. Note that the relative levels of significance are fairly consistent across subjects. **(B)** Histograms showing the time at which the significant broadband impulse responses reach their peak value, categorized by connection type. Because the electrodes were referenced in a bipolar manner, the peak value was measured as the maximum of the absolute value of the impulse response. Data from all 6 subjects are shown (dataset 1 = black, dataset 2 = gray), and histograms use 20ms bins. Here we see that the peak time for self-connections occurs in close proximity to the multi-unit spike (median = 16ms) as expected. The peak time for ISL connections is slightly delayed (median = 34ms). Most interesting are the CSL connections, which have a median peak time of 108ms after the multi-unit spike at time zero. Data from Subjects 1 and 2 are the primary contributors to this peak, although data from all six subjects are shown. This delay is presumably due to the complex, polysynaptic nature of the connection and the time needed to cross to the opposite hemisphere. Self-connections have been excluded from the ispilateral same lobe (ISL) category. All percentages are measured relative to the number of possible connections in that category, rather than the total number of all connections.

Key: CSL = contralateral same lobe (e.g. left temporal to right temporal), COL = contralateral other lobe (e.g. left temporal to right frontal), CSS = contralateral same structure (e.g. left amygdala to right amygdala), ISL = ipsilateral same lobe (e.g. between two left temporal structures), IOL = ipsilateral other lobe (e.g. left temporal to left frontal), Self = self-connections (within the same brain structure)

3.3 Amplitude-based impulse responses reveal same-lobe LFP activity tightly timed to MUA events

An analysis of the amplitude-based impulse response reveals additional relationships to spatial location and timing. First, the percentage of significant impulse responses is a function of both connection type and frequency (Figure 5A). The likelihood of a self-connection being significant rises steadily with frequency. The only other connections that could be regularly detected were between ipsilateral structures in the same lobe of the brain (excluding self-connections), with the highest percentage of significant connections occurring at 22.6 Hz (3.179%) and 32 Hz (3.165%). All other connection types were rare, with significance occurring much less than 1% of the time. This is in contrast to the impulse response based on the broadband LFP signal, where multiple connection types were detected. Similar results were seen on the level of individual subjects (Supplementary Figure 2).

Second, the peak of the amplitude-based impulse response is more tightly timed to the MUA, as compared to the broadband impulse response (Figure 5B, data shown for amplitude at 32Hz). Note the different horizontal axes in Figure 4B and Figure 5B; the peak of the amplitude-based impulse response generally occurs within 50ms of the multi-unit spike, while the broadband impulse response was spread over 500ms. As expected, the peak of the amplitude-based impulse response for self-connections is precisely timed to the MUA (Figure 5B, top left; median value 0ms). For ipsilateral connections (both same lobe and different lobe) and contralateral connections between left/right temporal lobe and left/right frontal lobe, the peak of the impulse response typically occurs within 6.2ms of the multi-unit spike (Figure 5B, top right and bottom row).

3.4 Significant impulse response measurements are related to the epileptogenic zone

When the data were pooled across all subjects, the likelihood of short and long distance connections mirrored anatomical connectivity; however, not all anatomically connected regions demonstrated a significant impulse response. Within individual subjects, the significant connections tended to be clustered within specific regions of the brain and were asymmetric across hemispheres. This suggests that the subject-level functional connections could reflect aberrant networks unique to each patient.

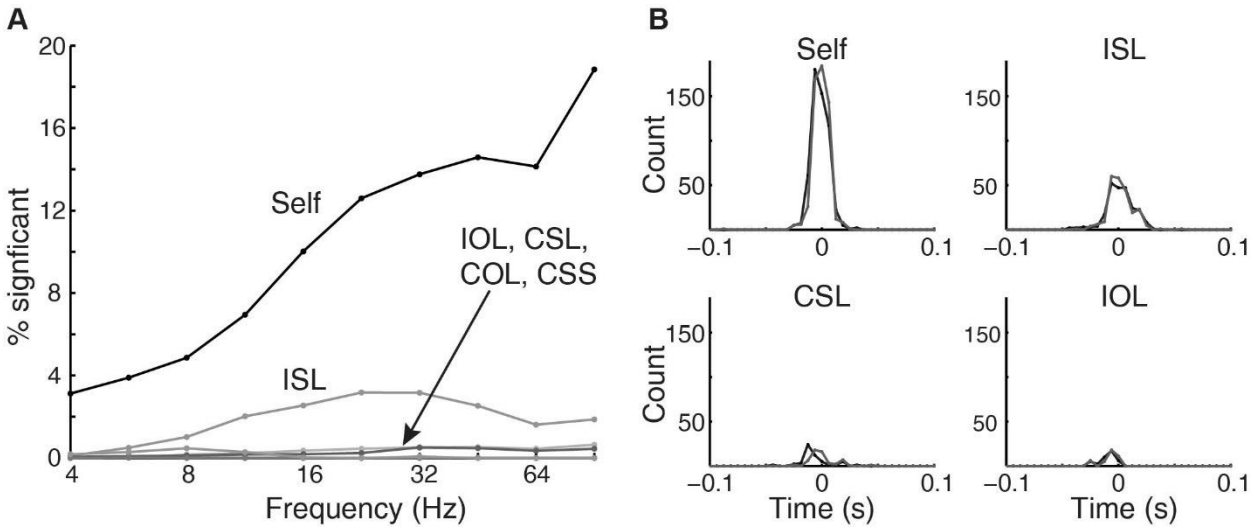

Figure 5. Significant amplitude-based impulse responses occur most often for self-connections and ISL connections and are tightly linked to spike time. (A) Total percentage of significant amplitude-based impulse responses as a function of frequency. Results are categorized by connection type (see Key in Figure 4) and calculated over all six subjects. ISL connections reach a peak level of significance at 22.6 Hz (3.179% of ISL connections), and all other connection types (IOL, CSL, COL, CSS) have very few significant values (<1%). **(B)** Histograms showing the time at which the significant 32Hz-amplitude impulse responses reach their peak value, categorized by connection type. The 32 Hz frequency was chosen in order to match the large number of significant ISL connections in Figure 5A and overall maximum number of significant connections in Figure 3. Data from all 6 subjects are shown (dataset 1 = black, dataset 2 = gray), and histograms use 6.3ms bins. Here we see that the impulse responses based on LFP amplitude at 32 Hz reach their peak value coincident with the multi-unit spike, regardless of the connection type. The median values are 0ms (Self), 3.1ms (ISL), -3.1ms (CSL), and -6.2ms (IOL). Note that the x-axis here is +/- 100ms, while the x-axis in Figure 4B is +/- 500ms.

In order to correlate the functional connectivity results to the seizure onset zone, we compared our results to the clinical results for each subject. Recordings from the clinical depth electrodes were used to determine the location where seizures began, which was required before surgical treatment could be offered to the subjects involved in this study. While localization of the seizure onset zone may identify a single anatomical structure, removal of multiple structures is common practice to maximize the likelihood of surgical success. The neuroimaging, localization, surgery, and outcome data for all patients is listed in Table 1.

Out of six subjects, two had unilateral mesial temporal lobe onsets and each underwent standard anteromesial temporal lobectomy (AMTL) that resulted in postsurgical seizure-free outcome. In

these cases, the clusters of significant interictal functional connections were associated with sites of seizure onset.

- Subject 1 had seizures that began in LA, LEC, and LH (see Table 1 for more details and a list of all abbreviations). The largest number of significant impulse responses occurred between structures in the left temporal lobe, specifically between LEC and LPHG (Figure 6). Connections between LH (LFP) and LPHG (MUA) were also present, as well as a strong inter-hemispheric connectivity between left and right PHG. However, compared to the number of connections within and between LEC and LPHG, much fewer were detected in LH, which was the site of MRI hippocampal sclerosis.

- Subject 5 had a seizure onset zone that included LEC, LH, and LA (see also Table 1). Interictal connectivity analysis found significant impulse responses between LEC and LH and also between LA (LFP) and LEC and LH (MUA) (Figure 7). Impulse response analysis detected relatively few significant functional connections in LA (MUA); similar to Subjects 1 and 3 (see below), this was the site of MRI lesion.

In the remaining four subjects, clinical seizure localization using intracranial recordings was more challenging. Two had multiple sites of seizure onset, whereas the other two required further intracranial studies with grid electrodes to localize the site(s) of seizure onset.

- Functional connectivity results from Subject 2 showed strong connections within and between the left and right frontal and mesial temporal lobes (Supplementary Figure 3), which was consistent with the bilateral frontal and temporal sites of seizure onset.

- Subject 3 had significant connections within the right temporal lobe (REC, RA, and RH), which was also the location of frequent interictal sharp wave discharges. Fewer significant connections were found between LPHG and LA (Supplementary Figure 4). Seizure activity began on the proximal contacts of depth electrodes positioned in left temporal lobe that indicated temporal neocortical seizure onset zone that required grid electrode studies to further localize site(s) of onset.

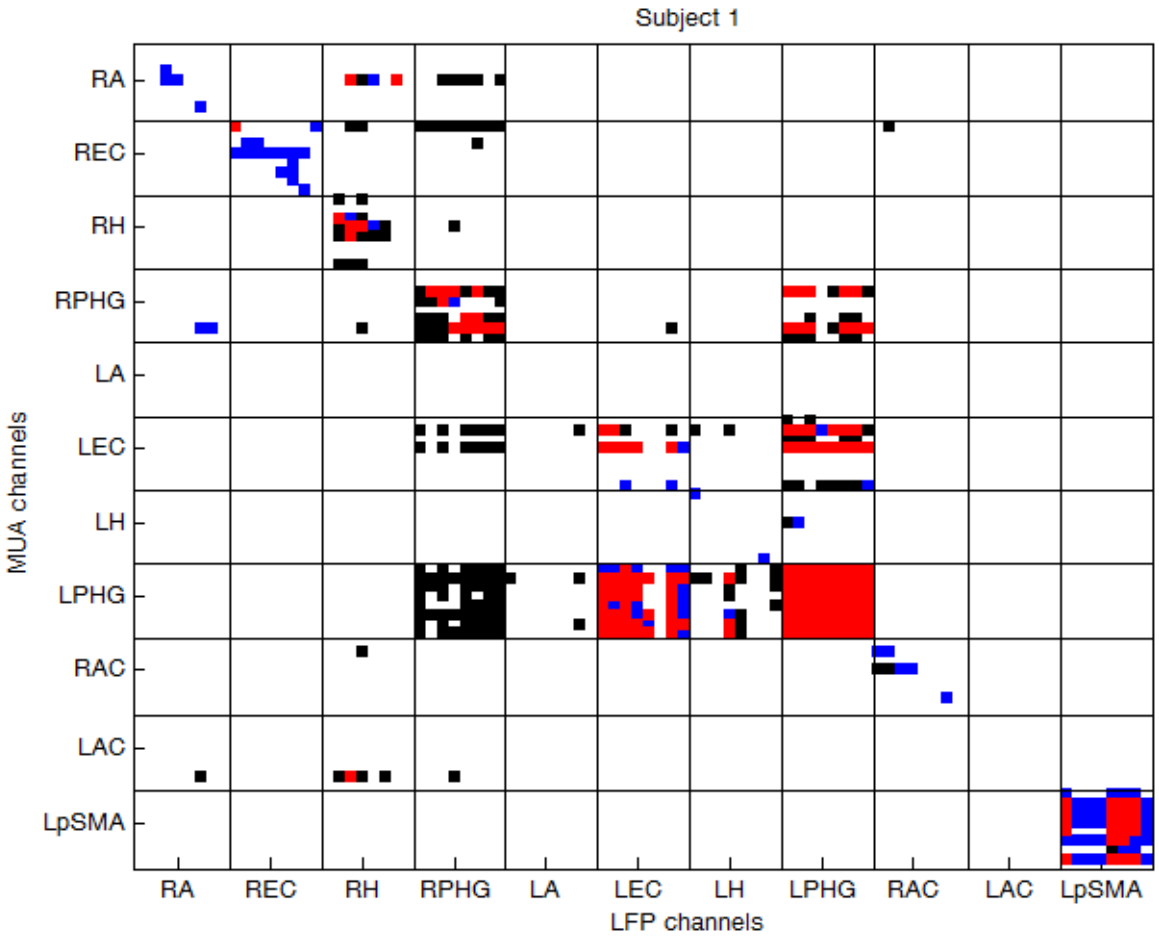

Figure 6. Significant functional connections for Subject 1. Here the vertical axis indicates the location of the MUA measurement (8 microwires per region) and the horizontal axis indicates the location of the LFP measurement (8 microwires per region). All pairs were tested. Black squares indicate impulse responses that were significant based only on the broadband LFP, and blue squares denote significance for the amplitude-based measure only. Red squares indicate a significant impulse response using both the broadband measure and the amplitude-based measure at one or more frequencies. Key: Prefix of R/L indicates right/left; A = amygdala, AC = anterior cingulate, H = hippocampus, EC = entorhinal cortex, PHG = parahippocampal gyrus, pSMA = pre-supplementary motor area.

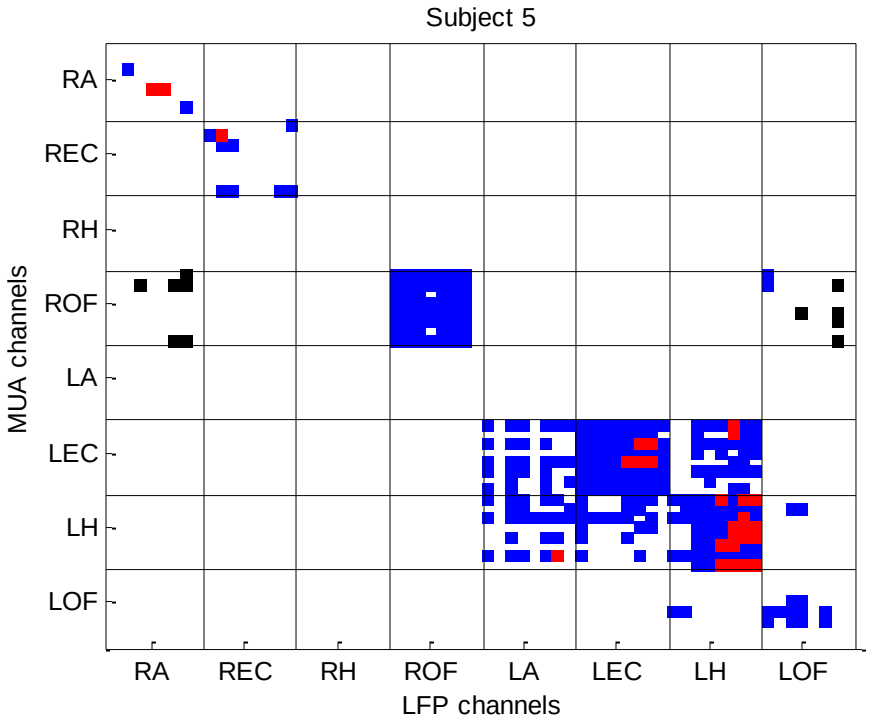

Figure 7. Significant functional connections for Subject 5. See Figure 6 for an explanation of axes and colors. This subject's seizures were localized to the left temporal lobe, with interictal epileptiform discharges in LEC and LH and seizure onset occurring most frequently in LEC, LH, and LA. Imaging showed left amygdala hypometabolism on PET and increased T2/FLAIR intensity on MRI. This subject underwent left AMTL and was seizure free five months after surgery. Key: Prefix of R/L indicates right/left; A = amygdala, H = hippocampus, EC = entorhinal cortex, OF = orbitofrontal.

- In Subject 4, impulse response analysis detected very few significant interictal functional connections in mesial temporal and frontal structures (Supplementary Figure 5). This patient had previously undergone resective surgery for epilepsy (left AMTL), and in the current study, depth electrodes positioned around the resection cavity and bilateral frontal lobe sites could not unequivocally identify the region were seizures began.
- Subject 6 had significant functional connections chiefly associated with the right superior temporal gyrus with sparse connectivity within and between right and left mesial frontal and left temporal structures (Supplementary Figure 6). Palliative resective surgery of seizure onset zone included anterior mesial and lateral temporal lobe, but did not include an area of probable polymicrogyria that encompassed inferior pre- and post-central gyri.

Results for all six subjects are summarized in Figure 8. Here we categorize the MUA/LFP recording location as left or right hemisphere and temporal or frontal lobe, and we count the

percentage of significant connections within and across each category. Overall, our analyses found several examples where the interictal spike-triggered impulse responses mirrored the clinical localization of the seizure onset zone. In two subjects with clear localization and a seizure-free surgical outcome, the brain regions with a large number of significant functional connections were a good match to the seizure onset zone and the locations of interictal epileptiform discharges. By contrast, in those cases where depth electrodes could not lateralize or localize the area of seizure onset, interictal connectivity also showed relatively few significant connections or bilateral connectivity. Lastly, our results also suggest a possible link to abnormal findings on MRI and PET, with the affected regions exhibiting very few significant functional connections based on the local MUA.

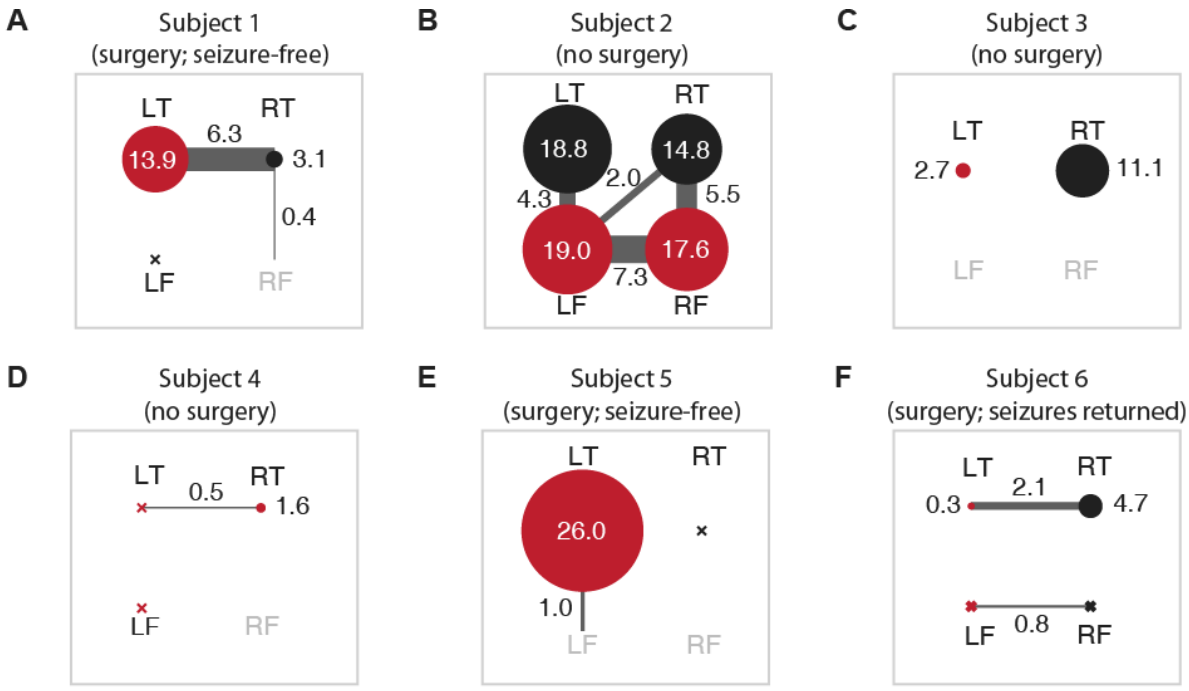

Figure 8. The network of significant impulse responses is unique to each patient and appears to be related to the epileptogenic zone. The diagrams show the percentage of significant impulse responses for each subject, categorized by spatial location of the MUA and LFP. Key: LT = left temporal, RT = right temporal, LF = left frontal, and RF = right frontal. Connections that were deemed significant by any measure (broadband, amplitude, or both) were counted here, and we do not consider the connections to be directional. All self-connections within a single structure have been excluded. A blank entry indicates that <0.05% of connections were significant, and a gray label indicates that this type of connection was not measured (e.g. only one structure in the right frontal lobe of subject 1 was measured and therefore only self-connections could be calculated). The lobes in which seizure onset occurred are colored red. In subjects 1 and 5, who had clear seizure localization and successful surgery, the locations

with the greatest percentages of significant connections were consistent with the clinical localization of the epileptic activity (Table 1).

4 Discussion

Here we have demonstrated that the neuronal spike-triggered impulse response can detect long-range functional connectivity in the epileptic human brain. The impulse response revealed a strong correlation between MUA and LFP from distinct brain structures, sometimes across hemispheres, and the results were reliable when tested on two independent datasets. Overall, the likelihood of detecting significant connections matched general properties of anatomical connectivity. For example, connections were most likely to occur between structures in the same lobe of the brain, and inter-hemispheric connections generally associated two analogous lobes or structures. Further, the timing of the impulse response was related to the connection type, with contralateral connections having longer delays than those between ipsilateral structures. However, in individual subjects with clear localization and seizure-free outcome, significant interictal functional connections were associated with the epileptogenic zone. While these results are preliminary due to the low number of subjects and the short follow-up period, the impulse response warrants further investigation as a valuable tool to identify and quantitatively evaluate pathological networks that support the generation of seizures.

The impulse response is related to the spike-triggered average of the LFP (Gregoriou et al., 2009; Jin et al., 2011; Nauhaus et al., 2009; Ray and Maunsell, 2011), but it removes the effects of spatiotemporal autocorrelations within the spike train (Einevoll et al., 2013). This type of calculation, which relates MUA and LFP activity, is common in animal studies. For example, the impulse response had previously been applied to local connectivity in the visual cortex of non-human primates (Nauhaus et al., 2012; Rasch et al., 2009). Here, calculation of the impulse response in humans is possible due to a unique opportunity to carry out direct microelectrode recordings in presurgical patients with medically resistant epileptic seizures.

There are two important points regarding interpretation of the impulse response. First, an estimate of the impulse response using correlation analysis does not, in principle, provide information about causality. This estimate is based on the cross-covariance between the multi-unit spike train and the LFP and does not include a minimum phase constraint. In some cases, we

found that the onset of the impulse response preceded the onset of MUA (Figure 2A, D), which could indicate that the LFP reflects input to presynaptic cells and the MUA corresponds to postsynaptic output. More complex signal processing techniques, such as Granger causality, directed transfer function, or partial directed coherence, are needed to confirm this directed functional connectivity. Alternatively, dynamic causal modeling could provide a measure of directed (effective) connectivity. Second, we treated each connection within the network as independent, and this is not necessarily the case. For example, a connectivity pattern of X→Y→Z would likely also give the result that X→Z. Multivariate analyses, such as conditional Granger causality, are able to distinguish between these two patterns and may clarify the full extent of each connection.

Results from our analysis showed impulse responses between MUA and LFP from the same brain structure were more likely to be significant than any other type of connection (Figure 4A), and the percentage of significant connections increased with frequency (Figure 5A). We cannot exclude the possibility that these local connections are due to contributions of the low-frequency component of neuronal spike waveforms to the LFP (Ray et al., 2008). Since we did not computationally remove or correct for the potential contamination of neuronal spikes to the LFP, the finding of significant local connections was expected, although we do not believe this could explain all significant connections for several reasons. It has been demonstrated that local neuronal spike-LFP correlations can be detected after careful removal of neuronal spikes from the LFP signal (Zanos et al., 2011), indicating that these relationships are robust, even in the presence of additional noise. Further, while an extracellular spike waveform can contain significant power below 200 Hz, a majority of this is between 100-200 Hz (Zanos et al., 2011). Here, both the broadband and amplitude-based analyses were restricted to frequencies under 100 Hz. Lastly, we would expect the presence of this low frequency power to have a similar effect on all channels, but the distribution of significant local connections was non-uniform across brain regions. Note that the low-frequency component of the spike waveform does not impact the calculation of the impulse response when the MUA and LFP come from different brain structures, so no other results are affected.

We expect that the impulse response will be equally useful as a measure of functional connectivity in animal and human studies, in both healthy and diseased conditions. For example, it may be possible to observe changes in the connectivity in different cognitive states if the

network is driven by different stimuli or tasks. However, the significant functional connections measured in this study appear to be related to the epileptogenic network rather than normal, cognitive processes. There are three reasons we believe this to be the case: First, the connections between brain regions are sparse and asymmetric. Most MUA/LFP comparisons did not yield significant connections (note the prevalence of white squares in Figures 6 and 7), and the asymmetry between the left and right hemispheres was striking (Figures 6, 7, and 8). Second, the pattern of significant impulse responses was unique for each patient. In brain regions that were measured across more than one subject, the associated connectivity patterns varied; for example, compare the results for the left hippocampus (LH) MUA in subject one (Figure 6) and subject five (Figure 7). Third, the ability to assess the functional connectivity in each subject appeared to be linked to the success of the clinical seizure localization. In cases where there was clear, unilateral localization and seizure-free surgical outcome, the impulse response analysis showed strong functional connections in regions of seizure onset and interictal epileptiform discharges.

These results are related to other studies of large-scale functional connectivity in epilepsy. In agreement with previous work, we found that interictal electrophysiological data could be used to infer information about the epileptogenic zone (Bartolomei et al., 2013; Bettus et al., 2011; Kramer et al., 2011). The reported characteristics of seizure-specific connectivity have varied. Some have found an increase in local connectivity ipsilateral to the seizure onset zone (Bartolomei et al., 2013; Haneef et al., 2014; Luo et al., 2014; Maneshi et al., 2014), while others have reported decreased local connectivity (Bettus et al., 2009; Maccotta et al., 2013; Morgan et al., 2012; Pittau et al., 2012; Weaver et al., 2013). There seems to be more consistency in the question of long-distance connectivity, where the epileptogenic zone has been found to be less connected to the contralateral hemisphere, the default mode network, and sensorimotor networks (Bartolomei et al., 2013; Luo et al., 2014; Maccotta et al., 2013; Voets et al., 2012). At the same time, there is evidence that contralateral local connectivity is increased, possibly as a way of compensating for damage within the epileptogenic zone (Bettus et al., 2009; Morgan et al., 2012). Here we find that, in two subjects with clear clinical localization, a large percentage of significant functional connections occur in the same lobe as the epileptogenic zone and many of those are in regions associated with seizure onset. On the other hand, brain regions in the seizure onset zone that were abnormal based on imaging findings appeared to be associated with very few significant functional connections. This is possibly consistent with reports of compensatory connectivity; for example, in subject 1, left hippocampal atrophy is associated with a lack of

functional connections, but the surrounding connections of the entorhinal cortex and parahippocampal gyrus are strong.

In spite of the limited spatial sampling associated with the standard bilateral depth electrode placements used in these subjects, impulse response analysis detected several significant functional connections consistent with the epileptogenic zone (subjects 1 and 5). It is possible that this approach, combined with the higher spatial sampling typically achieved with a stereotactic EEG approach or high density hybrid grid electrodes, could provide additional information to more accurately delineate the brain areas responsible for generating seizures. Impulse response analysis could also be used to study the characteristics of specific functional connections between two brain regions across patients grouped by seizure onset, e.g. interaction between the hippocampus and amygdala in patients with left temporal lobe seizure onset. It may also shed light on the relationship between functional connectivity and imaging findings, such as a comparison of hippocampal functional connectivity in patients with and without hippocampal sclerosis. Lastly, as discussed above, we expect that this technique could be applied more broadly to studies of cognition in both humans and animals.

Overall, the impulse response appears to be a promising technique for the measurement of functional connectivity. Using human data, we have demonstrated the ability to detect long-range connections and shown preliminary evidence of the relationship to the seizure onset zone. This analysis does not rely on the measurement of seizures, which can be infrequent and unpredictable, and used only twenty minutes of interictal data. Future work will include a larger clinical study, which will enable a detailed analysis of the characteristics and state-dependence of functional networks across subjects and etiologies.

Table 1. Clinical data for the subjects included in the study

Sub-ject	Years since epilepsy onset	MRI findings	PET findings	Interictal activity	Ictal onset location (# of seizures)	Resection	Post-surgical seizures (# of months)
1	45.5	Left hippocampus increased T2/FLAIR signal intensity	Left mesial temporal hypometabolism	---	LEC, LH (1) LA, LEC, LH (5)	Left anteromesial temporal lobectomy (LAMTL)	0 (9 mos.)
2	42	No significant findings	Right temporal pole hypometabolism	Synchronous discharges RSMA & LSMA	RSMA, LSMA (3); RpSMA, LpSMA (9)	---	N/A
3	20	Mild bilateral hippocampal atrophy	Bilateral temporal lobe hypometabolism	Sharp wave discharge REC; slowing LEC,LH; infrequent sharp wave discharges, LH, LEC, LPHG, RA	LEC (1); LH, LPHG (4); LA (1)	---	N/A
4	14	Mild increased FLAIR signal adjacent to previous LAMTL margins	No significant findings	---	LPHG, LAC, LMC, LpSMA (7); RH, RPT (6); Bilateral (1)	(prior LAMTL)	N/A
5	53	Left amygdala increased FLAIR signal intensity	Left amygdala hypometabolism	EEG spikes LEC, LH	LEC, LH, LA (5); LA (2)	LAMTL	0 (5 mos.)
6	19	Polymicrogyria left lateral frontal operuculum	Right temporal lobe hypometabolism	EEG spikes left lateral temporal lobe	LEC (1); LEC, LH (1); LMC (4); LH (1); LCLF (1); LMC, LCLF (3)	Left anterolateral & superior temporal	1 (3 mos.)

Key: Prefix of R/L indicates right/left; suffix of a/p indicates anterior/posterior; A = amygdala, AC = anterior cingulate, EC = entorhinal cortex, H = hippocampus, MC = middle cingulate, PHG = parahippocampal gyrus, (p)SMA = (pre) supplementary motor area, PT = posterior temporal

Acknowledgements

RJS was supported by NINDS R01 5NS071048. We would like to thank Eric Behnke and Tony Fields for technical assistance and Nanthia Suthana for electrode localizations.

References

Bartolomei, F., Bettus, G., Stam, C.J., and Guye, M. (2013). Interictal network properties in mesial temporal lobe epilepsy: a graph theoretical study from intracerebral recordings. Clinical neurophysiology : official journal of the International Federation of Clinical Neurophysiology *124*, 2345-2353.

Bettus, G., Guedj, E., Joyeux, F., Confort-Gouny, S., Soulier, E., Laguitton, V., Cozzone, P.J., Chauvel, P., Ranjeva, J.P., Bartolomei, F*., et al.* (2009). Decreased basal fMRI functional connectivity in epileptogenic networks and contralateral compensatory mechanisms. Human brain mapping *30*, 1580-1591.

Bettus, G., Ranjeva, J.P., Wendling, F., Benar, C.G., Confort-Gouny, S., Regis, J., Chauvel, P., Cozzone, P.J., Lemieux, L., Bartolomei, F*., et al.* (2011). Interictal functional connectivity of human epileptic networks assessed by intracerebral EEG and BOLD signal fluctuations. PloS one *6*, e20071.

Cash, S.S., and Hochberg, L.R. (2015). The emergence of single neurons in clinical neurology. Neuron *86*, 79-91.

Einevoll, G.T., Kayser, C., Logothetis, N.K., and Panzeri, S. (2013). Modelling and analysis of local field potentials for studying the function of cortical circuits. Nature reviews Neuroscience *14*, 770-785.

Engel, A.K., Moll, C.K., Fried, I., and Ojemann, G.A. (2005). Invasive recordings from the human brain: clinical insights and beyond. Nature reviews Neuroscience *6*, 35-47.

Engel, J., Jr., Thompson, P.M., Stern, J.M., Staba, R.J., Bragin, A., and Mody, I. (2013). Connectomics and epilepsy. Current opinion in neurology *26*, 186-194.

Fried, I., Rutishauser, U., Cerf, M., and Kreiman, G., eds. (2014). Single Neuron Studies of the Human Brain (MIT Press).

Gregoriou, G.G., Gotts, S.J., Zhou, H.H., and Desimone, R. (2009). High-Frequency, Long-Range Coupling Between Prefrontal and Visual Cortex During Attention. Science *324*, 1207-1210.

Haneef, Z., Lenartowicz, A., Yeh, H.J., Engel, J., Jr., and Stern, J.M. (2012). Effect of lateralized temporal lobe epilepsy on the default mode network. Epilepsy & behavior : E&B *25*, 350-357.

Haneef, Z., Lenartowicz, A., Yeh, H.J., Levin, H.S., Engel, J., Jr., and Stern, J.M. (2014). Functional connectivity of hippocampal networks in temporal lobe epilepsy. Epilepsia *55*, 137-145.

Holmes, M., Folley, B.S., Sonmezturk, H.H., Gore, J.C., Kang, H., Abou-Khalil, B., and Morgan, V.L. (2014). Resting state functional connectivity of the hippocampus associated with neurocognitive function in left temporal lobe epilepsy. Human brain mapping *35*, 735-744.

Jin, J., Wang, Y., Swadlow, H.A., and Alonso, J.M. (2011). Population receptive fields of ON and OFF thalamic inputs to an orientation column in visual cortex. Nat Neurosci *14*, 232-238.

Keller, C.J., Truccolo, W., Gale, J.T., Eskandar, E., Thesen, T., Carlson, C., Devinsky, O., Kuzniecky, R., Doyle, W.K., Madsen, J.R*., et al.* (2010). Heterogeneous neuronal firing patterns during interictal epileptiform discharges in the human cortex. Brain : a journal of neurology *133*, 1668-1681.

Kramer, M.A., Eden, U.T., Lepage, K.Q., Kolaczyk, E.D., Bianchi, M.T., and Cash, S.S. (2011). Emergence of persistent networks in long-term intracranial EEG recordings. The Journal of neuroscience : the official journal of the Society for Neuroscience *31*, 15757-15767.

Luo, C., An, D., Yao, D., and Gotman, J. (2014). Patient-specific connectivity pattern of epileptic network in frontal lobe epilepsy. NeuroImage Clinical *4*, 668-675.

Maccotta, L., He, B.J., Snyder, A.Z., Eisenman, L.N., Benzinger, T.L., Ances, B.M., Corbetta, M., and Hogan, R.E. (2013). Impaired and facilitated functional networks in temporal lobe epilepsy. NeuroImage Clinical *2*, 862-872.

Maneshi, M., Vahdat, S., Fahoum, F., Grova, C., and Gotman, J. (2014). Specific resting-state brain networks in mesial temporal lobe epilepsy. Frontiers in neurology *5*, 127.

Morgan, V.L., Sonmezturk, H.H., Gore, J.C., and Abou-Khalil, B. (2012). Lateralization of temporal lobe epilepsy using resting functional magnetic resonance imaging connectivity of hippocampal networks. Epilepsia *53*, 1628-1635.

Nauhaus, I., Busse, L., Carandini, M., and Ringach, D.L. (2009). Stimulus contrast modulates functional connectivity in visual cortex. Nat Neurosci *12*, 70-76.

Nauhaus, I., Busse, L., Ringach, D.L., and Carandini, M. (2012). Robustness of traveling waves in ongoing activity of visual cortex. The Journal of neuroscience : the official journal of the Society for Neuroscience *32*, 3088-3094.

Pesaran, B., Pezaris, J.S., Sahani, M., Mitra, P.P., and Andersen, R.A. (2002). Temporal structure in neuronal activity during working memory in macaque parietal cortex. Nat Neurosci *5*, 805-811.

Pittau, F., Grova, C., Moeller, F., Dubeau, F., and Gotman, J. (2012). Patterns of altered functional connectivity in mesial temporal lobe epilepsy. Epilepsia *53*, 1013-1023.

Rasch, M., Logothetis, N.K., and Kreiman, G. (2009). From neurons to circuits: linear estimation of local field potentials. The Journal of neuroscience : the official journal of the Society for Neuroscience *29*, 13785-13796.

Ray, S., Hsiao, S.S., Crone, N.E., Franaszczuk, P.J., and Niebur, E. (2008). Effect of stimulus intensity on the spike-local field potential relationship in the secondary somatosensory cortex. The Journal of neuroscience : the official journal of the Society for Neuroscience *28*, 7334-7343.

Ray, S., and Maunsell, J.H. (2011). Network rhythms influence the relationship between spike-triggered local field potential and functional connectivity. The Journal of neuroscience : the official journal of the Society for Neuroscience *31*, 12674-12682.

Swadlow, H.A., Gusev, A.G., and Bezdudnaya, T. (2002). Activation of a cortical column by a thalamocortical impulse. The Journal of neuroscience : the official journal of the Society for Neuroscience *22*, 7766-7773.

Voets, N.L., Beckmann, C.F., Cole, D.M., Hong, S., Bernasconi, A., and Bernasconi, N. (2012). Structural substrates for resting network disruption in temporal lobe epilepsy. Brain : a journal of neurology *135*, 2350-2357.

Weaver, K.E., Chaovalitwongse, W.A., Novotny, E.J., Poliakov, A., Grabowski, T.G., and Ojemann, J.G. (2013). Local functional connectivity as a pre-surgical tool for seizure focus identification in non-lesion, focal epilepsy. Frontiers in neurology *4*, 43.

Womelsdorf, T., Fries, P., Mitra, P.P., and Desimone, R. (2006). Gamma-band synchronization in visual cortex predicts speed of change detection. Nature *439*, 733-736.

Wyler, A.R., Ojemann, G.A., and Ward, A.A. (1982). Neurons in Human Epileptic Cortex - Correlation between Unit and Eeg Activity. Annals of neurology *11*, 301-308.

Zanos, T.P., Mineault, P.J., and Pack, C.C. (2011). Removal of spurious correlations between spikes and local field potentials. J Neurophysiol *105*, 474-486.